Ocean Engineering 145 (2017) 1–14

Contents lists available at ScienceDirect

Ocean Engineering

journal homepage: www.elsevier.com/locate/oceaneng

On the spatial dependence of extreme ocean storm seas

Emma Ross [a], Monika Kereszturi [b], Mirrelijn van Nee [c], David Randell [d], Philip Jonathan [a,*]

[a] Shell Projects and Technology, London SE1 7NA, United Kingdom
[b] Department of Mathematics and Statistics, Lancaster University, Lancaster LA1 4YW, United Kingdom
[c] Faculty of Electrical Engineering, Mathematics and Computer Science, Technical University of Delft, 2628 CD Delft, The Netherlands
[d] Shell Projects and Technology, 1031 HW Amsterdam, The Netherlands

ARTICLE INFO

Keywords:
Extreme
Spatial
Dependence
Max-stable process
Composite likelihood
Pooling
North Sea

ABSTRACT

Contemporaneous occurrences of extreme seas at multiple locations in a neighbourhood can cause greater structural reliability and human safety concerns than extremes at a single location. Understanding spatial dependence of extreme seas is important therefore in metocean design, yet has received little rigorous attention in the offshore engineering literature. We characterise the spatial dependence of storm peak significant wave height using three models motivated by max-stable processes for locations in the northern North Sea. Models for marginal extremes per location, and dependence of extremes between locations, are estimated using Bayesian inference with composite spatial likelihoods. We show that, in addition to marginal directional non-stationarity of extreme seas per location, all three models indicate spatial anisotropy in extremal dependence quantified by the spatial covariance matrix of the corresponding max-stable process. Estimates suggest that extreme seas show greater extremal dependence from West to East than from North to South.

1. Introduction

Extreme value analysis is a framework to characterise and quantify extreme phenomena. Using extreme value analysis, we estimate the marginal tail distribution of a single random variable, or the joint tail distribution of two or more random variables. Compared with marginal analysis, multivariate extreme value analysis is more challenging, less developed theoretically, and less used in practice.

One approach to multivariate extreme value analysis of oceanographic and engineering interest uses spatial processes to describe the behaviour of spatially-distributed extremes. Consider significant wave height (H_S) from wind-driven sea states over a spatial lattice of locations for intervals of time corresponding to storm events. We observe maxima of H_S per location per storm, referred to as storm peaks, and assume these to be independent in time. We are interested in characterising the spatial distribution of storm peak H_S. If the lattice consists of locations $1, 2, \ldots, p$, and the continuous random variables and values observed are respectively X_j, x_j, for $j = 1, 2, \ldots, p$, then the joint spatial density of storm peak H_S might be written $f(x_1, x_2, \ldots, x_p) = \partial^p F / \partial x_1 \partial x_2 \ldots \partial x_p$ evaluated at $(x_1, x_2, \ldots, x_p)$, where $F(x_1, x_2, \ldots, x_p) = \Pr[X_1 \leq x_1, X_2 \leq x_2, \ldots, X_p \leq x_p]$ is the joint cumulative distribution function. Assume now that H_S achieves a large maximum value (exceeding some threshold u_k) at some location k on the lattice. Then the conditional density

$$f(x_1, x_2, \ldots, x_p | X_k = x_k > u_k)$$

describes the "spatial shape" of dependence for a typical extreme storm. We might expect that spatial shape is dependent on characteristics of the environment: location (fetch, water depth, bathymetry) and wind field (central pressure, speed, direction, gradients, wind field spatial extent). We know from the literature (e.g. Mendez et al., 2008; Sartini et al., 2015) that marginal extreme value characteristics of H_S are non-stationary with respect to covariates such as wave direction and season. We might surmise therefore that storm shape varies with storm direction and season, as well as varying between ocean basins. When the data sample is sufficiently large, statistical models whose parameters are functions of covariates are generally necessary. In practical application, there may be insufficient evidence in the sample to identify and hence justify incorporating non-stationarity, especially for the spatial dependence structure. Ascertaining whether a typical North Sea hindcast sample shows evidence for non-stationarity of spatial dependence structure is the main objective of this work.

* Corresponding author.
E-mail address: philip.jonathan@shell.com (P. Jonathan).

http://dx.doi.org/10.1016/j.oceaneng.2017.08.051
Received 10 April 2017; Received in revised form 20 June 2017; Accepted 24 August 2017
Available online xxxx

We can write the joint density $f(x_1, x_2, \ldots, x_p)$ as the product of marginal densities $f(x_1), f(x_2), \ldots, f(x_p)$ and a dependence function $\mathcal{C}(x_1, x_2, \ldots, x_p)$

$$f(x_1, x_2, \ldots, x_p) = [f(x_1)f(x_2)\ldots f(x_p)]\mathcal{C}(x_1, x_2, \ldots, x_p).$$

Estimating the marginal densities is familiar territory: for each k, the tail $X_k > u_k$ can be estimated using a marginal extreme value model, and the density below u_k estimated empirically. Estimating the dependence function $\mathcal{C}$ is more problematic, especially when the values of one or more variables is extreme: spatial extreme value methods are needed. Note that spatial dependence is characterised by $\mathcal{C}$ only: if we transform each variable X_j to Y_j, such that $\{Y_j\}$ has a common marginal distribution, the corresponding transformed dependence function $\mathcal{C}_Y(y_1, y_2, \ldots, y_p)$ is a copula function. There is a large number of copula functions available to describe multivariate distributions, but only so-called extreme value copulas are appropriate to describe multivariate extreme value distributions (see Section 3).

From an engineering perspective, improved quantification of spatial dependence of extreme storms would allow better estimation of uncertainties in return values from analysis of spatially-pooled data; this is particularly relevant for ocean basins where storm events (hurricanes, tropical cyclones) have relatively low rates of occurrence over a spatial neighbourhood. The work of Heideman and Mitchell (2009) provides a valuable introduction to approaches used by practising metocean engineers for hurricane-type applications, including site averaging, grid point pooling and track shifting. The usual approach to uncertainty quantification of return values from spatially-pooled data is to assume (wrongly) that data from different locations are mutually independent; this is called the "independence likelihood" assumption (e.g. Chandler and Bate, 2007) leading to a joint density

$$f(x_1, x_2, \ldots, x_p) \approx f(x_1)f(x_2)\ldots f(x_p),$$

which ignores dependence function $\mathcal{C}$. We effectively assume that there are more independent observations than is actually the case, and therefore underestimate uncertainties during maximum likelihood estimation. To correct this, we then need to inflate uncertainty bands using a spatial "block bootstrapping" scheme (e.g. Chavez-Demoulin and Davison, 2005). Adopting a sample likelihood which more adequately represents extremal dependence would avoid the need to make the independence likelihood assumption. An approximation for the sample likelihood with captures spatial dependence of extremes is essential if Bayesian inference is to be used, since bootstrapping makes little sense in a Bayesian context. A better description of spatial shape would also improve our ability to quantify the consequences of extreme seas impacting multiple locations at the same time.

Max-stable process (MSP) models (following from the work of de Haan and Resnick, 1977) represent the most reasonable statistical approach currently available to inference for spatial extremes. MSPs can be thought of as extensions of multivariate extreme value distributions to continuous space, as summarised in Section 3. Their finite p-dimensional distributions provide a description of dependence function $\mathcal{C}$ above for a lattice of locations. Ribatet (2013) provides a review of MSPs, outlining the so-called Smith, (1990), Schlather, (2002) and Brown-Resnick (Brown and Resnick, 1977) models which have found some application in the environmental science literature. These models are described further in Section 3.2 and the Appendix, and will be applied in Section 5. Ribatet (2013) also provides an overview of methods for simulating from MSPs. Since the multivariate likelihood characterising extremal dependence cannot be written in closed form except in the bivariate case, approximate likelihoods are necessary for inference using maximum likelihood estimation. Padoan et al. (2010) presents a composite likelihood-based approximation for fitting MSPs, evaluates its performance using simulated data, and applies it to spatial extremes of daily precipitation. The composite likelihood framework used in this work is outlined in Section 4.

As MSPs arise as the limit distribution of componentwise maxima, they should be applied to samples of (contemporaneous) maxima (per location per time interval) for a lattice of spatial locations. However, extreme value inference using temporal peaks over threshold exploits the sample more efficiently. Following the ideas of Smith et al. (1997), Huser and Davison (2014) presents an approximate censored likelihood scheme for spatial modelling of peaks over threshold, used in this work also, as outlined in Section 4.

Different forms of extremal dependence exist, as outlined by Eastoe et al. (2013). Models based on consideration of componentwise maxima typically assume a particular form of extremal dependence, known as asymptotic dependence, as discussed e.g. by Kereszturi et al. (2016) for a sample of significant wave heights similar to that used in this work. This amounts to the assumption $\lim_{y\to\infty}\Pr[Y_l > y | Y_k > y] > 0$ at all pairs k, l of locations with Y_k, Y_l on common marginal scale (unless Y_k, Y_l are perfectly independent in which case the limit is 0). However, it is usually very difficult if not impossible to identify the form of extremal dependence present in a typical sample of limited size, with covariate effects also in play. Kereszturi et al. (2016) seek to refine the way diagnostics for extremal dependence are used in practice to improve their interpretability. For relatively large samples of sea state H_S, they find some evidence for asymptotic independence of extreme values between locations; for smaller samples of storm peak H_S, diagnostics are inconclusive. For this reason, we choose here to report applications of asymptotic dependent models (Section 5), whilst referring to related work (Kereszturi, 2016) for models exhibiting asymptotic independence yielding very similar results.

Estimation of spatial extremes models for samples of non-stationary peaks over threshold is complicated by at least three effects. Firstly, spatial extremes models are usually defined for block maxima not peaks over threshold; yet statistical inference is more efficient using peaks over threshold, and inference using peaks over threshold is commonplace in ocean engineering. Fortunately, for exceedances of a high threshold, likelihoods for block maxima and peaks over threshold can be shown to be approximately equal, so that the spatial extremes model can also be applied to peaks over threshold. However, we also need to model whole samples; we therefore apply a censored likelihood argument to construct approximate whole sample likelihoods for spatial extremes of peaks over threshold. Secondly, full joint distributions for spatial extremes are not available in closed form, but expressions for bivariate cumulative distribution functions and densities typically are. Using these, we need to construct composite likelihood approximations to the full likelihood for parameter estimation. Thirdly, spatial extremes models are defined assuming common standard Fréchet marginal distributions. In reality, marginal distributions are non-stationary with respect to covariates. We therefore need to fit non-stationary marginal models and transform marginally to standard Fréchet scale under these models. The spatial extremes model may of course also be sensitive to covariates.

The MSP is by far the most popular approach in the statistics literature to characterise extreme spatial processes. However, the conditional extremes model of Heffernan and Tawn (2004) provides an alternative modelling framework motivated by extreme value theory, advantageous in that it admits both asymptotic dependence and asymptotic independence within the same model. It also provides a relatively straightforward means for estimation on spatial grids, as illustrated e.g. by Eastoe et al. (2013).

1.1. Outline of paper

The motivation for this work is to consider (a) the feasibility and (b) the usefulness of applying multivariate extreme value models to real-world ocean engineering design problems. We assess the extent to which there is evidence, in typical samples of (storm peak) significant wave height where marginal non-stationarity has already been

accommodated, for non-stationarity or anisotropy in spatial dependence structures: how sophisticated a dependence model can typically be justified? As discussed in the next section, storm peak significant wave height data for a lattice of locations in the northern North Sea, similar to that previously presented by Kereszturi et al. (2016), is considered.

The article proceeds as follows. Following a description of the motivating North Sea application in Section 2, Section 3 provides an introduction to modelling spatial extremes using max-stable processes, and gives the cumulative distribution functions corresponding to the Smith, Schlather and Brown-Resnick models considered in this work. Complimenting Section 3, the Appendix gives an overview of the constructive representation of max-stable processes, and describes how sample realisations from the difference processes may be simulated. Section 4 provides an overview of the inference procedure used in this work, and addresses the majority of the complicating effects mentioned in the paragraph preceding this outline. In Section 5, we apply the spatial extremes models to the North Sea data. Conclusions are drawn in Section 6.

2. Data

2.1. Locations

We consider winter storm data from the NEXTRA hindcast (Oceanweather, 2002) for a lattice of 150 locations in the northern North Sea as shown in Fig. 1. Storm intervals for a total of 1680 storms (occurring in winter months October–March, common to all locations) during the period 1 Oct 1964 to 31 Mar 1995 were isolated from up- and down-crossings of a sea state significant wave height threshold for the central location. Storm peak significant wave height for each storm interval at each location provided a sample of 1680×150 observations for further analysis. For each storm-location combination, the direction (from which waves emanate, measured clockwise from North) at the time of the storm peak, referred to as the storm direction, was also retained. A plot of storm peak H_S on storm direction for the central location is shown in Fig. 2(a).

Fig. 1(a) shows the "bicycle wheel" of central transects through a common centre location, each (coloured) transect with a different spatial orientation. In Section 5, we will seek to quantify whether the spatial dependence of storm peak H_S along a transect varies systematically with the transect's orientation ϕ. Fig. 1(b) highlights the central transects with approximate West-East orientation, together with one of its parallel transects (with the same orientation). In Section 5 we will also examine whether the location of a transect of given orientation affects the spatial dependence of extreme storm severity along it.

2.2. Preprocessing

A key step in estimating an extremal dependence model is marginal modelling and subsequent transformation of data for each location to a standard scale. This is achieved, independently per location, by estimating a non-stationary marginal directional model following the approach of Ross et al. (2017), as described further in Section 4. Transformed data then follow the standard Fréchet distribution for each location. A plot of standardised storm peak H_S on storm direction for the central location is shown in Fig. 2(b). The effect of the land shadow of Norway for directions $\approx (30,\ 70)$ is relatively clear. There is some evidence for increased rate of occurrence of storm seas from approximately the South (for directions $\approx (180,\ 220)$) and North ($\approx (340,\ 20)$).

2.3. Dependence

Fig. 3 illustrates the spatial variation of storm peak H_S for 8 typical events from the sample. White discs indicate spatial maxima in each case, and the colour scheme indicates reduction in H_S to the spatial minimum, a black disc in each panel, as described in the figure caption. Panel (a) shows an event centred approximately in the middle of the grid from Fig. 1, decaying radially. The peak value for the event illustrated in panel (b) is probably actually outside the grid considered to the West. Panels (d) and (e) show events which are spatially more spread than that in panel (a). There appear to be two different storm processes contributing the panel (g), one from the North-West and one from the South-East; there may also be different storm processes contributing to each of panels (c) and (d).

We might expect that the dependence between pairs of standardised values for storm peak H_S for the same storm at two different locations would vary with the displacement of the locations. Fig. 4 shows that this is indeed the case. For neighbouring locations on the transects with angles $\phi = 4.6$ and -72.2 in panels (a) and (c) respectively, there is high dependence between standardised storm peak values of H_S as might be expected. Dependence is considerably lower when comparing standardised storm peak H_S values for the most distant pair of locations on each of those transects in panels (b) and (d).

3. Models

We consider three models for the spatial dependence of storm peak significant wave height. These are the Smith, Schlather and Brown-Resnick models. All have corresponding max-stable process (MSP) formulations exhibiting asymptotic dependence. In this section, we provide a brief introduction to max-stable processes, and describe the bivariate cumulative distribution functions corresponding to the three models.

3.1. Max-stable processes and distributions

The max-stable process (MSP) $Y(s)$ defined continuously on some spatial domain $\mathcal{S}$ ($\subseteq \mathbb{R}^2$ in our case, indexed by longitude and latitude) emerges as the limiting form of the maximum of independent and identically distributed random processes $\widetilde{Y}_i(s)$, $i = 1,\ 2,\ \ldots,\ n$, defined on $\mathcal{S}$, as described e.g. by Wadsworth and Tawn (2012) or Davison et al. (2012). For some sequence of continuous functions $\{a_n(s) > 0\}$ and $\{b_n(s)\}$,

$$\frac{\max_{i=1}^{n}\left\{\widetilde{Y}_i(s)\right\} - b_n(s)}{a_n(s)} \rightarrow Y(s) \text{ as } n \rightarrow \infty, \text{ for all } s \in \mathcal{S}$$

provided the limit exists, and $Y(s)$ has non-degenerate finite-dimensional distributions. Specifically, at any fixed location in $\mathcal{S}$ (indexed by k, say), the univariate distribution F_{Y_k} of Y_k is max-stable in the sense that $F_{Y_k}^n(b'_{kn} + a'_{kn}y_k) = F_{Y_k}(y_k)$ for some sequences $\{a'_{kn} > 0\}$ and $\{b'_{kn}\}$. Remarkably, the only possible choice for F_{Y_k} with this max-stable property is the generalised extreme-value (GEV) distribution

$$\begin{aligned} F_{Y_k}(y_k) &= \exp\left[-\exp\{(y_k - \eta)/\tau\}\right] \text{ for } \xi = 0, \\ &= \exp\left[-\{1 + \xi(y_k - \eta)/\tau\}_+^{-1/\xi}\right] \text{ otherwise,} \end{aligned}$$

with parameters: shape ξ, scale τ and location η. Moreover, the joint p-dimensional distribution F_Y for a lattice of p locations in $\mathcal{S}$ is max-stable with $F_Y^n\left(b'_{1n} + a'_{1n}y_1, b'_{2n} + a'_{2n}y_2,\ \ldots,\ b'_{pn} + a'_{pn}y_p\right) = F_Y\left(y_1,\ y_2,\ \ldots,\ y_p\right)$ for sequences $\{a'_{jn} > 0\}$ and $\{b'_{jn}\}$.

MSPs can thus be thought of as theoretical justification for a means of extending the GEV distribution for modelling of maxima at one location, to multivariate extreme value distributions for modelling of componentwise maxima observed on a grid of locations. At each location k, it is often convenient to transform Y_k to $Z_k = \{1 + \xi(Y_k - \eta)/\tau\}^{1/\xi}$ so that Z_k has a marginal unit Fréchet distribution $F_{Z_k}(z_k) = \exp(-1/z_k)$, for $z_k > 0$. With this transformation, the joint distribution (or copula) F_Z now has the special homogeneity property that

$$F_Z(z_1, z_2, \ldots, z_p) = \Pr[Z_1 \le z_1, Z_2 \le z_2, \ldots, Z_p \le z_p]$$
$$= \Pr\left[\frac{Z_1}{n} \le z_1, \frac{Z_2}{n} \le z_2, \ldots, \frac{Z_p}{n} \le z_p\right]^n \text{ by homogeneity}$$
$$= F_Z(nz_1, nz_2, \ldots, nz_p)^n.$$

Only choices of F_Z exhibiting this homogeneity correspond to finite-dimensional distributions from MSPs, and are hence valid for spatial extreme value modelling.

Exponent measure: It is conventional to express the joint distribution $F_Z(z_1, z_2, \ldots, z_p)$ in terms of an exponent measure $V_Z(z_1, z_2, \ldots, z_p)$ such that

$$F_Z(z_1, z_2, \ldots, z_p) = \exp\{-V_Z(z_1, z_2, \ldots, z_p)\}$$

with marginal identities $V_Z(z, \infty, \infty, \ldots, \infty) = V_Z(\infty, z, \infty, \ldots, \infty) = \ldots = V_Z(\infty, \infty, \ldots, \infty, z) = 1/z$ and homogeneity $V_Z(tz_1, tz_2, \ldots, tz_p) = t^{-1}V_Z(z_1, z_2, \ldots, z_p)$ for $t > 0$. The MSP models examined in Section 3.2 correspond to different choices of exponent measure.

Extremal coefficient: The exponent measure evaluated at $z_k = 1$ for all k provides a useful univariate summary of the dependence structure since

$$F_Z(z, z, \ldots, z) = \exp(-V_Z(z, z, \ldots, z))$$
$$= \exp(-z^{-1}V_Z(1, 1, \ldots, 1)) \text{ from the homogeneity property}$$
$$= \exp(-\theta_p/z)$$

where $\theta_p = V_Z(1, 1, \ldots, 1)$ is called the extremal coefficient. Upper and lower bounds for θ_p are p and 1 as outlined in the Appendix. The value of θ_p between p and unity indicates the extent of extremal dependence. For any pair of locations indexed by k, l, the extremal coefficient θ_{kl} also has a natural interpretation in terms of conditional bivariate exceedances and the asymptotic dependence diagnostic χ_{kl}, namely

$$\lim_{z\to\infty} \Pr[Z_l > z | Z_k > z] = 2 - \theta_{kl} = \chi_{kl},$$

as outlined in the Appendix. For the Smith, Schlather and Brown-Resnick MSP models used in this work, the bivariate exponent measure V_{kl} for all pairs of locations is available in closed form for Fréchet margins, facilitating maximum likelihood inference using a composite likelihood, as discussed in Section 4. We estimate the extremal coefficient of significant wave height for pairs of North Sea locations in Section 5 corresponding to different choices of MSP models.

3.2. Exponent measures

The bivariate exponent measures for the Smith, Schlather and Brown-Resnick MSPs, available in closed form, are described next. The constructive representation of MSPs, useful for simulating from the Smith, Schlather and Brown-Resnick models, is outlined in the Appendix.

Smith process: For any two locations s_k,s_l in $\mathcal{S}$, the exponent measure V_{kl} for the Smith process is given by

$$V_{kl}(z_k, z_l; h(\Sigma)) = \frac{1}{z_k}\Phi\left(\frac{m(h)}{2} + \frac{\log(z_l/z_k)}{m(h)}\right) + \frac{1}{z_l}\Phi\left(\frac{m(h)}{2} + \frac{\log(z_k/z_l)}{m(h)}\right),$$

where vector $h = s_l - s_k$, and $m(h)$ is the Mahalanobis distance between s_k and s_l, given by

$$m(h) = \left(h'\Sigma^{-1}h\right)^{1/2},$$

and Σ is a 2×2 covariance matrix. The value of $V_{kl}(1, 1; h(\Sigma))$ can be seen from its definition to be equivalent to $2\Phi(m(h)/2)$, providing a useful diagnostic check for simulations and assessment of dependence in exploratory analysis of data.

Schlather process: For any two locations s_k, s_l in $\mathcal{S}$, the exponent measure V_{kl} for the Schlather process is given by

$$V_{kl}(z_k, z_l; h(\Sigma)) = \frac{1}{2}\left(\frac{1}{z_k} + \frac{1}{z_l}\right)\left(1 + \left[1 - 2\frac{(\tau(h)+1)(z_k z_l)}{(z_k + z_l)^2}\right]^{1/2}\right)$$

where we choose to use the squared exponential correlation function $\tau(h) = \exp(-h'\Sigma^{-1}h)$ for covariance matrix Σ. The extremal coefficient $V(1, 1; h(\Sigma))$ is given by $1 + [(1 - \tau(h))/2]^{1/2}$, again useful as a diagnostic. Note that the extremal coefficient cannot reach 2 because $\tau(h) > 0$, so that the Schlather process cannot describe perfect independence for increasing h.

Brown-Resnick process: For any two locations s_k, s_l in $\mathcal{S}$, the exponent measure V_{kl} for the Brown-Resnick process takes the same form as that of the Smith process, with

$$m(h) = \sigma(h) = \left(h'\Sigma^{-1}h\right)^{H/2},$$

for Hurst parameter $H \in [0, 1]$. The Brown-Resnick process accommodates the whole range of values for the extremal coefficient (Davison et al., 2012). The Hurst parameter (or more generally the Hurst exponent) is a measure of long-term memory in stochastic processes, widely used in different branches of mathematics and physics. It is named after Harold Edwin Hurst (e.g. Sutcliffe (1979)), the British hydrologist who studied the characteristics of time series for the Nile basin's rain and drought conditions. A value of $H \in (0.5, 1)$ indicates long-range positive dependence, expected of the spatial characteristics of North Sea storm severity. $H \in (0, 0.5)$ indicates a tendency for long-term switching between high and low values for adjacent pairs.

3.3. Densities

Probability density functions f_{kl} corresponding to the exponent measures V_{kl} are required to construct likelihood expressions. These are obtained by straightforward but laborious differentiation

$$f_{kl}(z_k, z_l; h(\Sigma)) = \exp(-V_{kl})\left(\frac{\partial V_{kl}}{\partial z_k}\frac{\partial V_{kl}}{\partial z_l} - \frac{\partial^2 V_{kl}}{\partial z_k \partial z_l}\right)$$

where $V_{kl} = V_{kl}(z_k, z_l; h(\Sigma))$. Expressions for the Smith, Schlather and Brown-Resnick forms of f_{kl} are given in the Appendix.

3.4. Illustrations

Fig. 5 illustrates typical realisations from each of the Smith, Schlather and Brown-Resnick processes for different specifications of spatial covariance Σ (and Hurst parameter H for the Brown-Resnick processes). The realisations were generated using MATLAB algorithms written using the constructive representation and algorithms given in the Appendix. Parameter settings for Σ are specified in terms of the triplet (Σ_{11}, Σ_{22}, Σ_{12}). For larger values of Σ_{11}, Σ_{22} on the top row, realisations are generally smoother spatially, and obvious features are spatially more extensive. Reducing the Hurst parameter (final column) clearly also has an effect. Realisations of the Smith and Schlather process look more idealised, whereas the Brown-Resnick process appears to be producing realisations which are more plausible representations in general of physical processes. Comparison of the panels of Fig. 5 with those of Fig. 3 would suggest, assuming the spatial scales of the figures to be comparable, that panels (a)-(c) of Fig. 5 provide more realistic representations

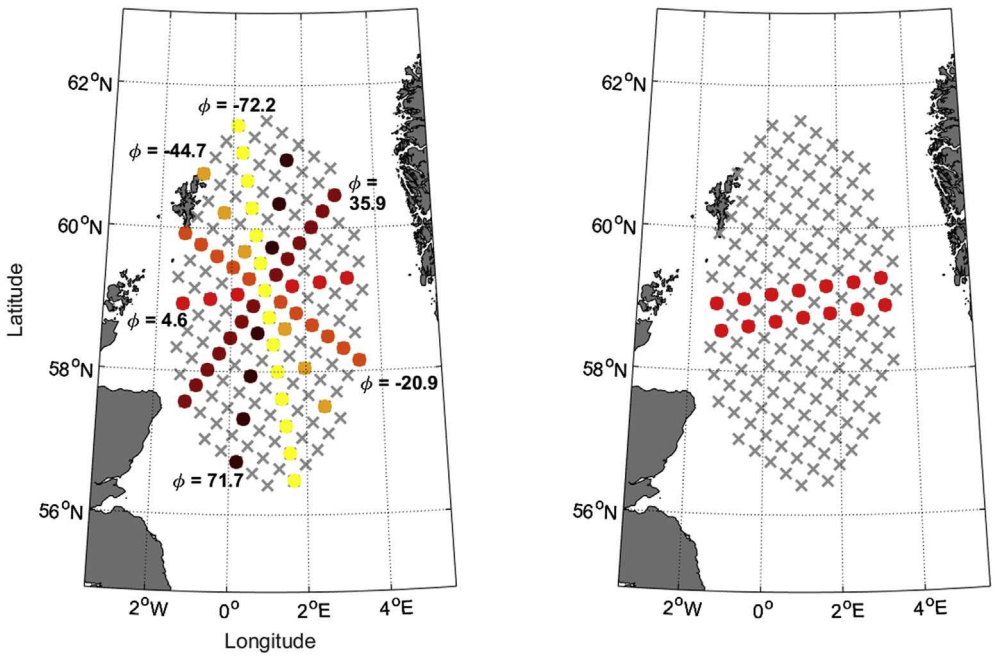

Fig. 1. Map of geographic locations examined. Panel (a) shows central transects for which extremal spatial dependence is estimated, colour-coded by orientation. Panel (b) shows the central red transect (with approximate West-East orientation) together with one (of a number) of its parallel transects. A set of parallel transects exists for each orientation. Note that the colour coding of transects in panel (a) corresponds to that of box-whisker plots in Figs. 6-8. (For interpretation of the references to colour in this figure legend, the reader is referred to the web version of this article.)

of the current sample. We also note that a higher value of Hurst parameter appears more plausible on this scale.

4. Estimation

This section explains the estimation procedure used. We start by outlining a composite likelihood for the spatial extremes model, assuming observations of peaks over threshold with standard Fréchet margins. Next we explain how to censor the bivariate distribution for block maxima on standard Fréchet margins, for which we have closed form expressions, so that it is also applicable to peaks over threshold on standard Fréchet margins. Then we give a brief description of the marginal analysis performed independently per location to transform samples to standard Fréchet scale. Finally, we give a step-by-step protocol for the Markov chain Monte Carlo estimation procedure used to estimate spatial extremes covariance matrix Σ, for each of the Smith, Schlather and Brown-Resnick models.

4.1. Composite likelihood

Suppose we have observations of peaks over threshold $\{y_j\}$ on standard Fréchet marginal scale at locations $\{s_j\} \in \mathcal{S}$. Since joint distributions for more than two locations are not available in closed form, we adopt a composite log likelihood

$$\ell_C(\Sigma; \{y_j\}) = \sum_{\{k,l\} \in \mathcal{N}} w_{kl} \log f_{kl}(y_k, y_l; h(\Sigma))$$

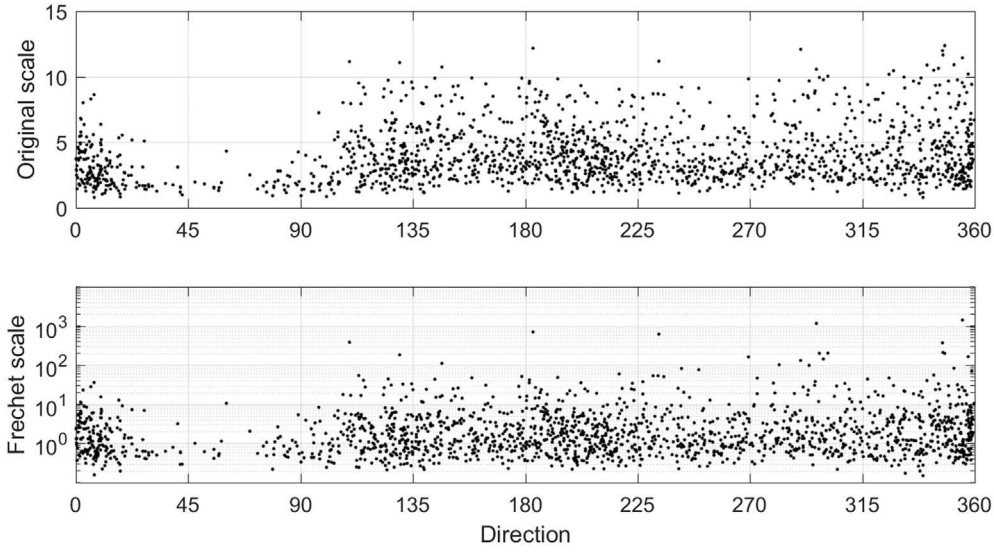

Fig. 2. Storm peak H_S on direction for central location (a) before and (b) after standardisation to Fréchet scale.

for covariance matrix Σ to be estimated, where $\{k, l\} \in \mathcal{N}$ indicates that locations s_k and s_l are neighbours, $\{w_{kl}\}$ are arbitrary weights, and f_{kl} is the corresponding bivariate density for peaks over threshold. Maximum likelihood estimates for Σ maximise $\ell_C(\Sigma;\ \{y_j\})$. In practice, all weights were set to unity, so that likelihood contributions from all pairs of locations were included.

4.2. Censored likelihood for peaks over threshold

The joint distribution of peaks over some high threshold u on standard Fréchet margins, Y_k, Y_l, can be related to the joint distribution of the corresponding block maxima on standard Fréchet margins, Z_k, Z_l, and hence the exponent measure. Following Huser and Davison (2014).

$$\begin{aligned}
\Pr[Y_k \le \mathrm{y_k}, Y_l \le \mathrm{y_l}] &= \left((\Pr[Y_k \le \mathrm{y_k}, Y_l \le \mathrm{y_l}])^2\right)^{1/2} \\
&= (\Pr[\max(Y_k, Y_l) \le \mathrm{y_k}, \max(Y_k, Y_l) \le \mathrm{y_l}])^{1/2} \\
&\approx \exp\left(-V_{kl}\left(\frac{\mathrm{y_k}}{2}, \frac{\mathrm{y_l}}{2}; h(\Sigma)\right)\right)^{1/2} \\
&\quad \text{if } \mathrm{y_k}, \mathrm{y_l} > u \quad \text{for some high threshold } u \\
&= \exp\left(-\frac{1}{2}V_{kl}\left(\frac{\mathrm{y_k}}{2}, \frac{\mathrm{y_l}}{2}; h(\Sigma)\right)\right) \\
&= \exp(-V_{kl}(\mathrm{y_k}, \mathrm{y_l}; h(\Sigma))) \\
&\quad \text{since V is homogeneous of order } -1, \\
&= \Pr[Z_k \le \mathrm{y_k}, Z_l \le \mathrm{y_l}]
\end{aligned}$$

That is, if both y_k and y_l are large, we can approximate the joint distribution of peaks over threshold by the corresponding distribution of block maxima, and use the densities from Section 3.3 directly to construct likelihoods for peaks over threshold modelling. However, we still need to construct an approximate likelihood for the case when one or both of z_k, z_l does not exceed u. For this purpose, we follow Huser and Davison (2014) in constructing a censored likelihood approximation for peaks over threshold defined as

$$f_{\mathrm{kl}}(\mathrm{y_k}, \mathrm{y_l}; \mathrm{h}(\Sigma)) = \begin{cases} \dfrac{\partial^2}{\partial \mathrm{y_k} \partial \mathrm{y_l}} \exp\{-V_{\mathrm{kl}}(\mathrm{y_k}, \mathrm{y_l}; \mathrm{h}(\Sigma))\}, & \mathrm{y_k}, \mathrm{y_l} > \mathrm{u}, \\ \dfrac{\partial}{\partial \mathrm{y_k}} \exp\{-V_{\mathrm{kl}}(\mathrm{y_k}, \mathrm{u}; \mathrm{h}(\Sigma))\}, & \mathrm{y_k} > \mathrm{u}, \mathrm{y_l} \le \mathrm{u}, \\ \dfrac{\partial}{\partial \mathrm{y_l}} \exp\{-V_{\mathrm{kl}}(\mathrm{u}, \mathrm{y_l}; \mathrm{h}(\Sigma))\}, & \mathrm{y_k} \le \mathrm{u}, \mathrm{y_l} > \mathrm{u}, \\ \text{and} & \\ \exp\{-V_{\mathrm{kl}}(\mathrm{u}, \mathrm{u}; \mathrm{h}(\Sigma))\}, & \mathrm{y_k}, \mathrm{y_l} \le \mathrm{u}. \end{cases} \tag{1}$$

Adopting this expression in the composite likelihood allows estimation of spatial extremes covariance matrix Σ, provided that the sample is available on standard Fréchet margins. We note, as discussed further in Section 6, that the pairwise composite likelihood is an approximation to the full likelihood. It is not equivalent to the full likelihood, and there is loss of information from adopting the pairwise composite likelihood approximation. Nevertheless, composite likelihood methods provide useful inferential tools when the full likelihood may not be available. An overview of composite likelihood methods is given by Varin et al. (2011).

4.3. Marginal analysis

Non-stationary marginal extreme value analysis using the piecewise gamma-generalised Pareto model of Ross et al. (2017), independently per location, is used to characterise the distribution of peaks over threshold of storm peak significant wave height with storm direction as a covariate. Quantile regression (for a fixed quantile threshold probability) is used to partition the sample prior to independent gamma (body) and generalised Pareto (tail) estimation. An ensemble of independent models, each member of which corresponds to a choice of quantile probability from a wide interval of quantile threshold probabilities, is estimated. Diagnostic tools are then used to select an interval of quantile threshold probabilities corresponding to reasonable model performance, for subsequent inference of extreme quantiles incorporating threshold uncertainty. The joint posterior distribution $f_M(\beta_M)$ of parameter estimates β_M is used to transform the original sample, independently per location, to standard Fréchet scale.

4.4. MCMC estimation

Markov chain Monte Carlo (MCMC) inference is used to estimate the joint distribution of the elements of spatial covariance matrix Σ. The adaptive Metropolis algorithm of Haario et al. (2001) discussed by Roberts and Rosenthal (2009), which automatically tunes the Markov chain parameters during execution, is adopted to propose parameters jointly. We proceed according to the algorithm below for each MCMC iteration r.

From the marginal analysis per location, samples of 10,000 points from the posterior distribution $f_M(\beta_M)$ of parameters β_M are available. For estimation of dependence covariance Σ, we use small perturbations of the maximum likelihood estimate as starting points for adaptive MCMC. Writing Ω for the triplet $[\Sigma_{11}, \Sigma_{22}, \Sigma_{12}]$, a starting value for each element ω of Ω is sampled from a uniform distribution centred at the corresponding maximum likelihood estimate ω_0 with half width 0.03 ω_0. Starting triplets corresponding to non-positive definite Σ are rejected. We then evolve multiple MCMC chains, one for each perturbation of the maximum likelihood estimate, and then compare trajectories post burn-in to confirm reasonable chain convergence.

Trajectories evolve as follows. At MCMC iteration r, candidates Ω_r^c are sampled according to

$$\Omega_r^c = \Omega_{r-1} + \gamma\varepsilon_1 + (1-\gamma)\varepsilon_2$$

where $\gamma \in [0, 1]$, $\varepsilon_1 \sim N(0, \delta_1^2 I_3/3)$, $\varepsilon_2 \sim N(0, \delta_2^2 S_{\Omega_{r-1}}/3)$, I_3 is the three-dimensional identity matrix and $S_{\Omega_{r-1}}$ is an estimate for the covariance matrix of Ω based on the values $\Omega_1, \Omega_2, \ldots, \Omega_{r-1}$. Following Roberts and

Algorithm MCMC iteration for spatial covariance Σ.

Input: Current state Σ_{r-1}, marginal posterior $f_M(\beta_M)$, original sample D of storm peak H_S.

Output: Updated state Σ_r.

1: Draw a set of marginal parameters β_{Mr} from f_M, independently per location.
2: Use β_{Mr} to transform D to standard Fréchet scale, independently per location, obtaining sample D_{Fr}.
3: Execute adaptive MCMC step from state Σ_{r-1} with sample D_{Fr} as input, obtain Σ_r.
4: **return** Σ_r.

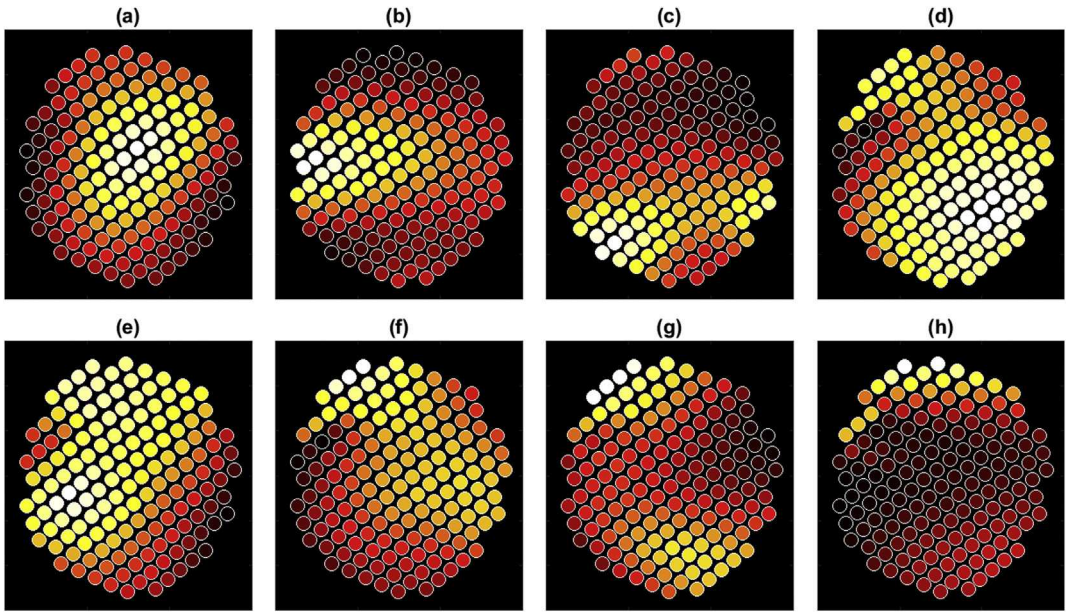

Fig. 3. Observations of the spatial distribution of storm peak H_S over the grid shown in Fig. 1 for 8 typical events (a)–(h). The spatial maximum for each event is given as a white disc, and the spatial minimum as a black disc (with white outline). The white → yellow → red → black colour scheme indicates the spatial variation of relative magnitude of storm peak H_S. (For interpretation of the references to colour in this figure legend, the reader is referred to the web version of this article.)

Rosenthal (2009) we set $\delta_1 = 0.1$ and $\delta_2 = 2.38$. We found it useful to use a value of $\gamma = 0.2$, larger than that recommended by Roberts and Rosenthal (2009), to produce candidates which explore the space of elements of Σ more freely. For the first few iterations, we use $\gamma = 1$. A Wishart prior is assumed for Σ, and parallel chains used to check MCMC convergence.

5. Application

The methods and procedures given in Sections 3 and 4 were used to estimate the spatial covariance Σ of storm peak H_S at the northern North Sea locations for the Smith, Schlather and Brown-Resnick models, using Bayesian inference. Estimates are illustrated for each model in turn in Figs. 6–8 in terms of the spatial dependence $\sigma(\phi)$ exhibited along transects with different orientations. For the Smith model, Fig. 6 shows both one-dimensional and two-dimensional estimates for $\sigma(\phi)$ along each of the transects illustrated in Fig. 1. Box-whisker plots illustrate 95% credible intervals for estimates for the (scalar) covariance Σ obtained by applying the one-dimensional Smith model to data from all transects with particular orientation only. Transect orientation is shown on the x-axis. Since inferences may be sensitive to the choice of the marginal extreme value threshold, and the censoring threshold for spatial modelling, estimates are presented for two choices of marginal threshold non-exceedance probability on rows 1 and 2, and two choices of censoring threshold non-exceedance probability in columns 1 and 2. Note that a larger set of combinations of marginal and censoring thresholds were examined, but results for only two threshold choices are illustrated in the text. Each panel also gives the corresponding estimate of spatial dependence obtained from estimating a two-dimensional Smith model for all locations. The spatial dependence $\sigma(\phi)$ along transect with orientation ϕ is estimated using

$$\sigma^2(\phi) = [\cos(\phi) \quad \sin(\phi)] \quad \Sigma \quad [\cos(\phi) \quad \sin(\phi)]^T.$$

It can be seen that 95% credible intervals from the two-dimensional model are narrower than from the one-dimensional model, but that the general characteristics of the one- and two-dimensional estimates for $\sigma(\phi)$ are in excellent agreement for all combinations of thresholds. Corresponding estimates for the Schlather and Brown-Resnick models are given in Figs. 7 and 8, showing excellent agreement with Fig. 6 in terms of general trends with orientation ϕ. A prior sensitivity study suggested that a choice of Hurst parameter $H = 0.75$ was appropriate. In this study, we evaluated the profile likelihood for the negative log composite likelihood as a function of H for the 2-D Brown-Resnick model using the full sample with marginal and dependence thresholds corresponding to non-exceedance probabilities of 0.65. A minimum log likelihood for $H \approx 0.75$ was observed. The choice of marginal and dependence model censoring thresholds clearly influences the estimates of $\sigma(\phi)$, with higher thresholds yielding weaker dependence. We emphasise that we estimated $\sigma(\phi)$ for all combinations of marginal and dependence thresholds $\in \{0.5, 0.65, 0.8\}$, and found that the general trends in $\sigma(\phi)$ to be similar throughout; for brevity, we chose to report results for only some of those combinations here. There is evidence from all figures that the estimate for spatial dependence $\sigma(\phi)$ is largest in an approximately West-East direction, and least in an approximately North-South direction. That is, the spatial similarity between extremes of storm peak significant wave height at these locations is greater from West to East than from North to South. This observation can be interpreted in terms of a model storm system propagating in a predominantly North-South (or South-North) direction, such that locations on the storm front (perpendicular to direction of propagation) exhibit higher spatial dependence of storm peak H_S than locations lying along the storm trajectory. This is at least physically plausible given the bathymetry of the northern North Sea. However, storm systems propagating predominantly West-East, such that locations on the storm front (perpendicular to direction of propagation) exhibit lower spatial dependence of storm peak H_S than locations lying along the storm trajectory, would also produce similar dependence structure.

The spatial dependence shown in Figs. 6–8 can also be illustrated in terms of the extremal coefficient $\theta = \theta_2$ defined in Section 3. This is particularly convenient because it allows direct comparison of the competing models. Results are given in Fig. 9 for the same four combinations of thresholds. For clarity, only one-dimensional estimates are reported; good correspondence between one- and two-dimensional estimates has already been established. Agreement between the Smith and Schlather estimates is excellent, with Brown-Resnick estimates somewhat higher. All estimates are in the region of 1.7, but estimates are lower for transects with orientations near zero. Recalling that θ_2 has domain [1,2], with 1 indicating perfect dependence and 2 perfect

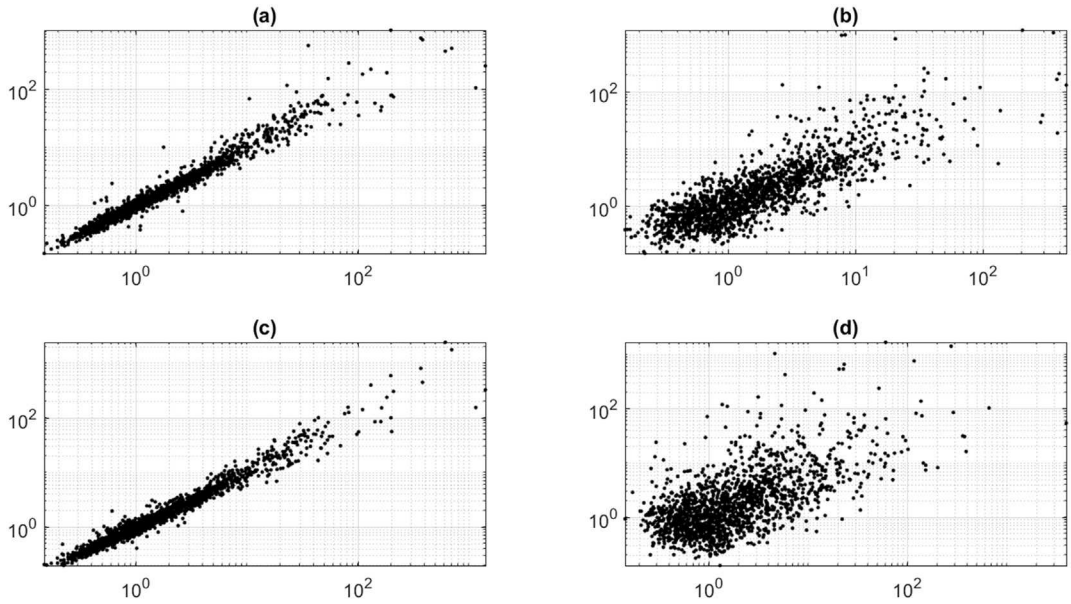

Fig. 4. Scatter plots of standardised storm peak H_S for different pairs of locations. Panel (a) for the central location and its nearest neighbour to the West along the approximate West-East transect with angle $\phi = 4.6$; panel (b) for the end locations of the same transect. Panel (c) for the central location and its nearest neighbour to the North along the approximate North-South transect with angle $\phi = -72.2$; panel (d) for the end locations of the same transect.

independence, we infer that transects with orientations near zero exhibit stronger dependence.

Next we examine the variability in spatial dependence for sets of parallel transects with a given orientation. The left-hand panel of Fig. 10 illustrates the five transects with different orientations ϕ, each considered as the first transect of a set with common orientation. As we move from the first transect ($s = 1$) with some orientation ϕ to its nearest parallel neighbour transect ($s = 2$) with the same orientation ϕ, the value of spatial dependence $\sigma(\phi, s)$ is illustrated in the right-hand panels. It appears that $\sigma(\phi, s)$ is lower for small s, namely transects near the Shetland Isles and Scotland, suggesting that spatial dependence between locations decays more quickly with distance here. Transects with moderate values for s, in the centre of the region explored, show higher values of $\sigma(\phi, s)$ in general, and hence higher spatial dependence between locations. These observations suggest a model with non-stationary Σ parameterised in terms of absolute location may provide an improved description of extremal spatial dependence.

6. Discussion

In this work we provide clear evidence for anisotropy in spatial dependence of extreme seas. For a neighbourhood of locations in the northern North Sea, we demonstrate that storm peak significant wave height varies with location and direction. We use marginal directional

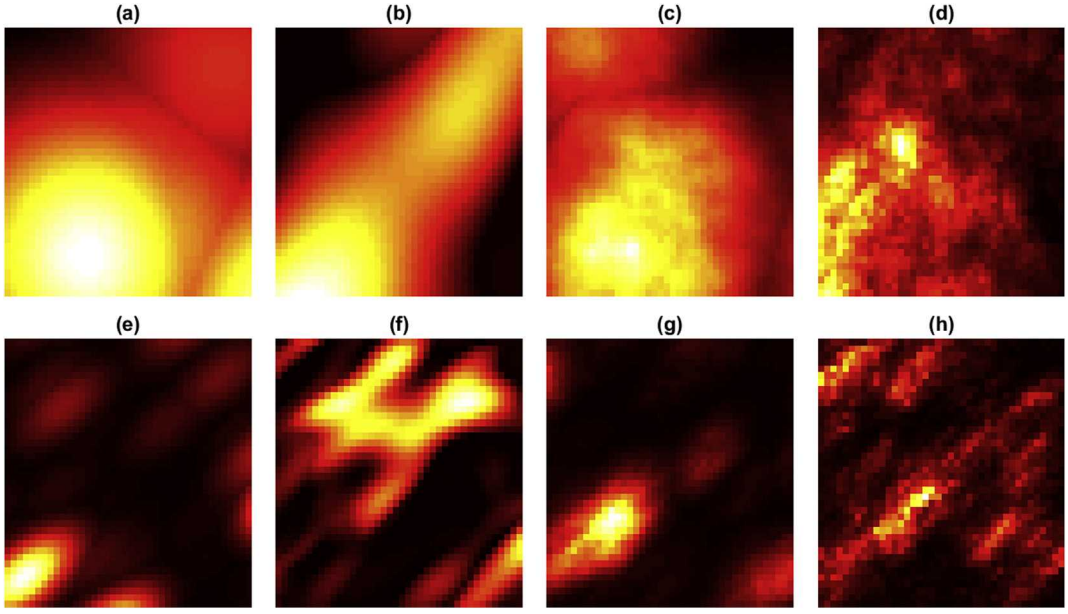

Fig. 5. Illustrative realisations of Smith (a, e), Schlather (b, f), and Brown-Resnick (c, d, g, h) processes for different parameter choices. The first row corresponds to parameter settings $(\Sigma_{11}, \Sigma_{22}, \Sigma_{12}) = (300, 300, 0)$ for all processes, and the second row to (30, 20, 15). For Brown-Resnick processes (c, g), Hurst parameter $H = 0.95$. For Brown-Resnick processes (d, h), $H = 0.65$. Each panel can be considered to show a possible spatial realisation of storm peak H_S, similar to those shown in Fig. 3. The colour scheme is the same as that used in Fig. 3. (For interpretation of the references to colour in this figure legend, the reader is referred to the web version of this article.)

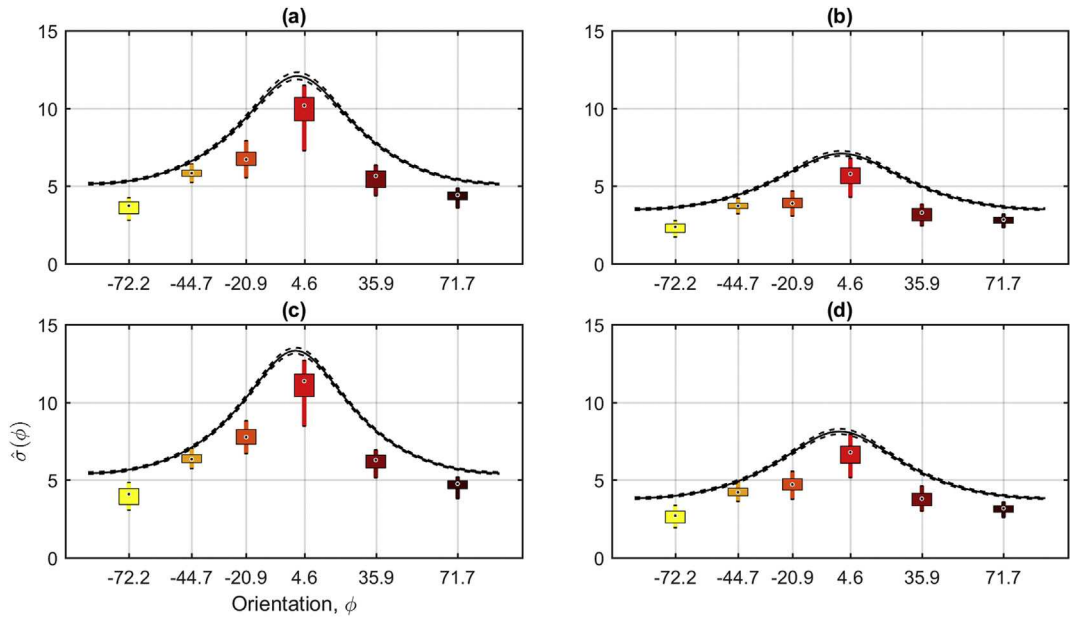

Fig. 6. Estimated extremal spatial dependence parameter $\hat{\sigma}(\phi)$ for all transects with a given orientation ϕ estimated using 1-D (box-whisker) and 2-D (black) Smith processes. ϕ is quantified as the transect angle anticlockwise from a line of constant latitude, as is apparent from comparison with Fig. 2. The first (second) row corresponds to a choice of marginal threshold with non-exceedance probability 0.5 (0.8). The first (second) column corresponds to a choice of censoring threshold with non-exceedance probability 0.5 (0.8). For 1-D estimates with a given ϕ, box centres corresponds to the median estimate, and box edges to the 0.25 and 0.75 quantiles across all parallel transects; whisker edges correspond to the 0.025 and 0.975 quantiles. For 2-D estimates, the 0.025, 0.5 and 0.975 quantiles are shown as a function of ϕ. Note that the colour coding of box-whisker plots corresponds to that of transect orientation in Fig. 1. (For interpretation of the references to colour in this figure legend, the reader is referred to the web version of this article.)

extreme value models, estimated independently per location, to characterise marginal non-stationarity. After accounting for marginal effects, there is still considerable remaining directional non-stationarity in the spatial dependence between extreme seas at different locations. The extent of West-East dependence is higher than that of North-South dependence.

Software in MATLAB and "R" was developed independently in parallel at Shell and Lancaster respectively to validate inferences. The MATLAB code was further validated by repeating the analysis of maximum composite likelihood estimation provided by Padoan et al. (2010). "R" code for the current analysis is available from the authors on request.

Choice of extremal dependence class for multivariate spatial extreme value modelling of significant wave height is problematic, due to the presence of covariate effects and typically limited sample size. Yet estimating the corresponding non-stationary marginal behaviour is

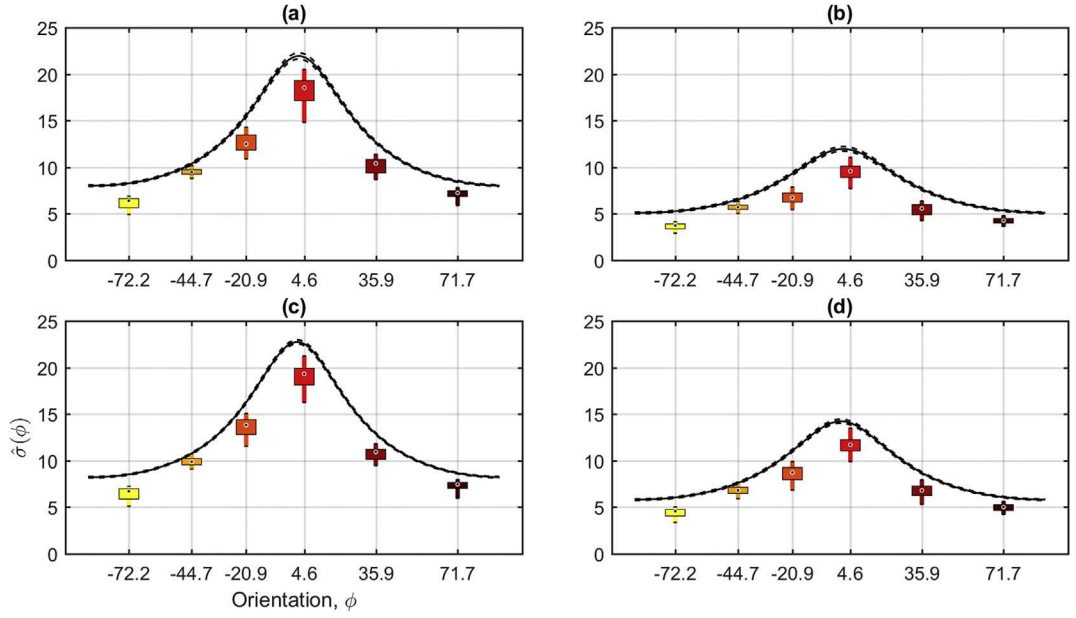

Fig. 7. Estimated extremal spatial dependence parameter $\hat{\sigma}(\phi)$ for all transects with a given orientation ϕ estimated using 1-D (box-whisker) and 2-D (black) Schlather processes. ϕ is quantified as the transect angle anticlockwise from a line of constant latitude, as is apparent from comparison with Fig. 2. The first (second) row corresponds to a choice of marginal threshold with non-exceedance probability 0.5 (0.8). The first (second) column corresponds to a choice of censoring threshold with non-exceedance probability 0.5 (0.8). Other details as for Fig. 6.

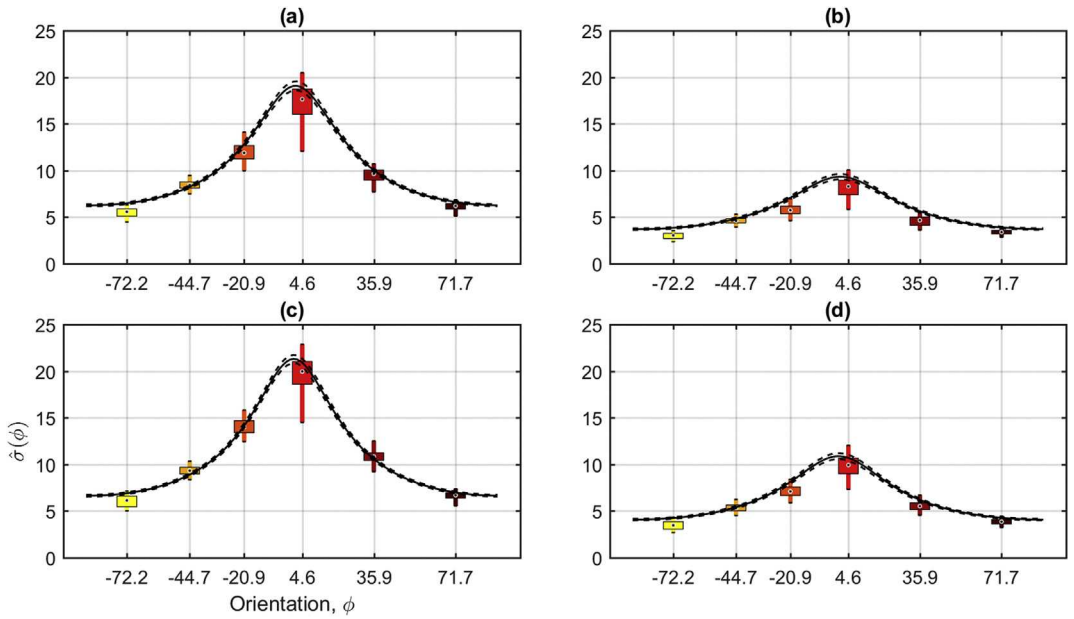

Fig. 8. Estimated extremal spatial dependence parameter $\widehat{\sigma}(\phi)$ for all transects with a given orientation ϕ estimated using 1-D (box-whisker) and 2-D (black) Brown-Resnick processes with $H = 0.75$. ϕ is quantified as the transect angle anticlockwise from a line of constant latitude, as is apparent from comparison with Fig. 2. The first (second) row corresponds to a choice of marginal threshold with non-exceedance probability 0.5 (0.8). The first (second) column corresponds to a choice of censoring threshold with non-exceedance probability 0.5 (0.8). Other details as for Fig. 6. (For interpretation of the references to colour in this figure legend, the reader is referred to the web version of this article.)

more straightforward due in large part to the existence of a unified (generalised extreme value) framework for marginal extremes. We therefore avoid the need to use different marginal specifications based on the value of the marginal shape parameter ξ ($\xi = 0$, Type I or Gumbel; $\xi > 0$, Type II or Fréchet; and $\xi < 0$, Type III or Weibull). Physical considerations, suggesting that the value of shape parameter may well be zero for some values of covariate, and negative or positive for others, make the unified framework highly advantageous in practical application of non-stationary extremes. Similarly, it seems likely that useable multivariate models bridging different extremal dependence classes, incorporating perfect dependence, asymptotic dependence, asymptotic independence and perfect independence in terms of

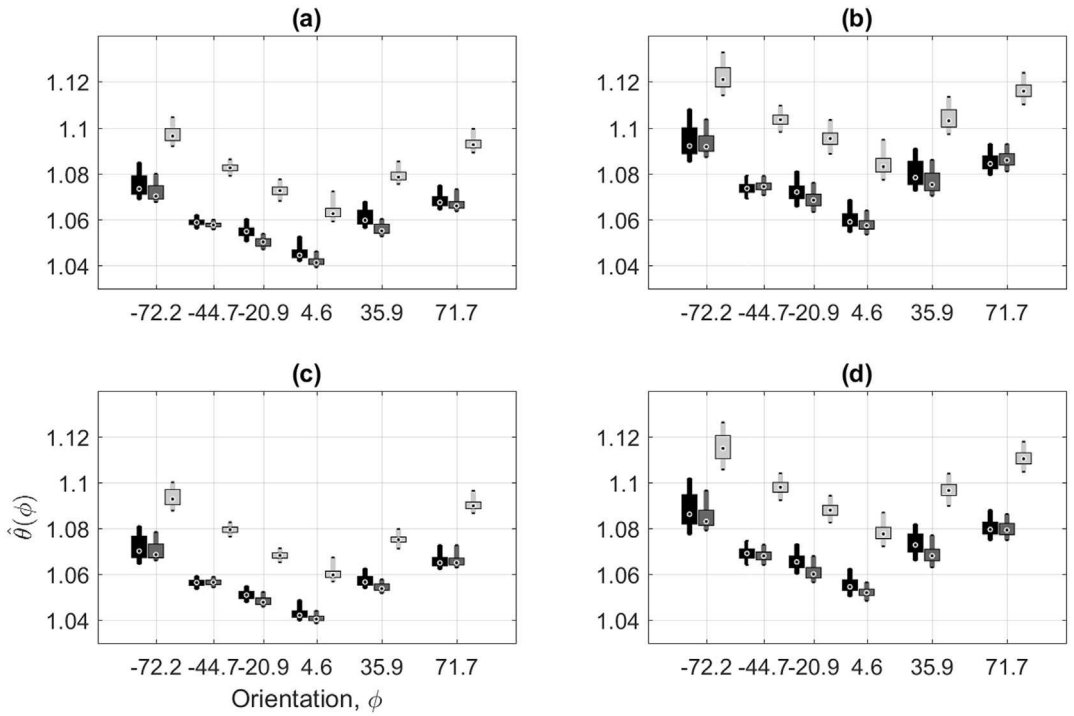

Fig. 9. Estimated extremal coefficient $\widehat{\theta}(\phi)$ for all transects with a given orientation ϕ, estimated using 1-D Smith (black), Schlather (dark grey) and Brown-Resnick (light grey) processes. The first (second) row corresponds to a choice of marginal threshold with non-exceedance probability 0.5 (0.8). The first (second) column corresponds to a choice of censoring threshold with non-exceedance probability 0.5 (0.8). For 1-D estimates with a given ϕ, box centres corresponds to the median estimate, and box edges to the 0.25 and 0.75 quantiles across all parallel transects; whisker edges correspond to the 0.025 and 0.975 quantiles.

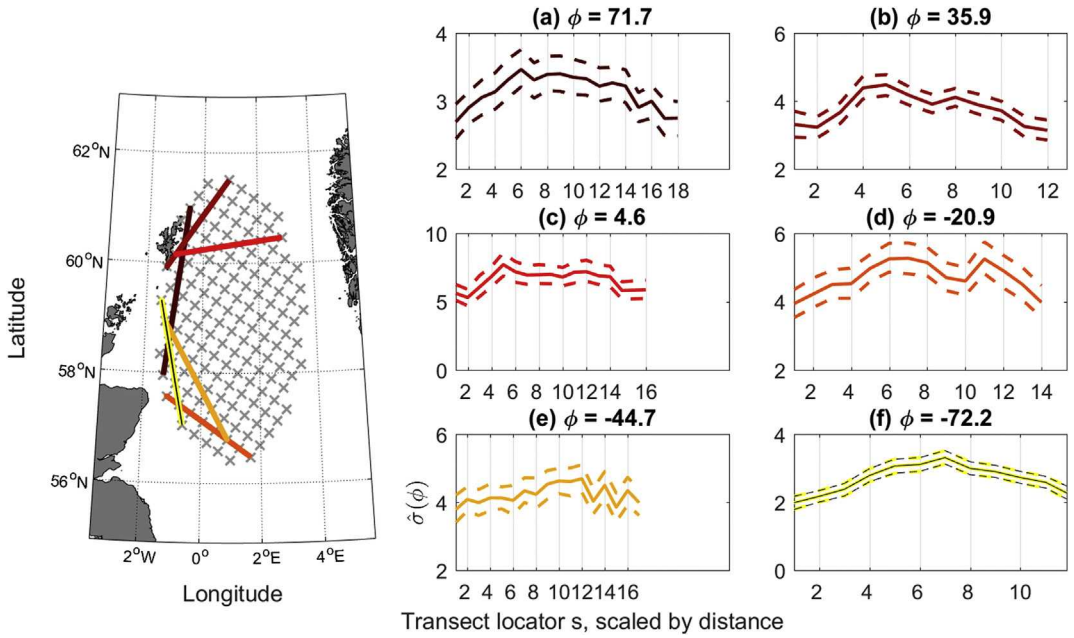

Fig. 10. Estimated extremal spatial dependence parameter $\hat{\sigma}(\phi, s)$ for individual transects, using a Smith process with marginal and censoring thresholds corresponding to a non-exceedance probability of 0.8. Each of panels (b)–(g) shows $\hat{\sigma}(\phi, s)$ for fixed orientation ϕ (given in the panel title) as a function of transect locator s. Panel (a) shows transects with $s = 1$ for different orientations ϕ. The sequence of subsequent parallel transects ($s = 2, 3, 4, \ldots$) for each orientation is defined in the obvious way. In panels (b)–(g), abscissa values for transect locators are scaled to physical perpendicular distances between parallel transects.

smooth variation of one or more model parameters, will emerge in the near future. These would facilitate flexible non-stationary modelling of extremal dependence structure, and effectively eliminate concerns about choice of dependence class. The work of Wadsworth et al. (2017) is a step in this direction.

We have only considered spatial models motivated by max-stable processes exhibiting asymptotic dependence. In related work, Kereszturi (2016) also considered asymptotically independent spatial processes for the North Sea data examined here, focussing again on estimation of the spatial covariance Σ. The characteristics of Σ observed using asymptotic independent models are very similar indeed to those of the asymptotic dependent models considered here.

In terms of parameters estimation, the 2×2 covariance matrix Σ specifies all of the Smith and Schlather processes, the Brown-Resnick process (for given Hurst parameter H), and all their asymptotically independent inverted counterparts. Flexibility of choice of H makes the Brown-Resnick process more general than the Smith process (which corresponds to $H = 1$.) The Brown-Resnick process also offers a greater range of asymptotic dependence than the Schlather process as noted in Section 3.2. Ideally, we would like to be able to determine which of these processes, if any, provide adequate descriptions of a typical metocean sample, and whether any of the descriptions is materially better than the others. It seems that we can answer the first query positively, since all of Smith, Schlather and Brown-Resnick given reasonable descriptions of the current sample, and provide estimates for Σ and functions thereof with similar characteristics. Unfortunately, choosing the best description is difficult given the size of sample available here, and typically available in metocean applications. Model comparisons via criteria such as CLIC (composite likelihood information criterion, Padoan et al., 2010) have been considered by us, but these are generally not conclusive. Moreover, the elements of Σ are probably non-stationary with respect to numerous covariates, complicating parameter estimation and fair model comparison further.

It is obviously beneficial to use the framework of max-stable processes to describe spatial extremes, particularly in comparison to the assumption of spatial independence and adoption of an independence likelihood with block bootstrapping to correct uncertainty estimates. It has however been shown that use of composite likelihoods for max-stable models can lead to underestimation of uncertainties in spatial extremes models. Huser and Davison (2014) propose the use of three-component and higher-order likelihood contributions instead of bivariate to reduce this effect.

Threshold specification is difficult, even for marginal extreme value analysis. To implement marginal extremes inference reliably for offshore design, some of us recommend (as in Ross et al., 2017) that an ensemble of models for different threshold choices (possibly corresponding to threshold non-exceedance probabilities sampled from some "prior" distribution of plausible values) are used together for inference. Similarly, for reliable spatial extremes applications, it is likely that employing an ensemble approach over plausible choices of marginal and censoring thresholds will be useful. Reasonable choices of threshold combinations could be identified by examining the stability of key responses with respect to arbitrary combinations of plausible thresholds, as in the current study.

The current work has demonstrated spatial anisotropy for extreme storm peak significant wave height consistent with physical intuition. We have not investigated whether there is further evidence for non-stationarity of Σ with respect to covariates such as storm direction; this is a topic for future investigation. Other future steps might include simultaneous marginal and dependence inference, and simulation of spatial events under the fitted model. It would also be of interest to investigate whether evidence for spatial anisotropy exists in measured (particularly satellite) data for the North Sea, and in data for other ocean basins.

Acknowledgement

We are grateful to Kevin Ewans of Metocean Solutions Limited (New Zealand) for providing motivation and expertise on this and related projects over many years. We thank Graham Feld and Vadim Anokhin of Shell and Jonathan Tawn of Lancaster University for useful discussions.

Appendix

Bounds for the extremal coefficient

In the notation of Section 3.1, when components Z_k are independently Fréchet distributed, we have $F_Z(z_1, z_2, \ldots, z_p) = F_{Z_1}(z_1)F_{Z_2}(z_2) \ldots F_{Z_p}(z_p)$ and hence $V_Z(z_1, z_2, \ldots, z_p) = \sum_{k=1}^{p} 1/z_k$. Hence $\theta_p = V_Z(1, 1, \ldots, 1) = p$. When components Z_k are completely dependent, $F_Z(z_1, z_2, \ldots, z_p) = F_{Z_k}(\min(z_1, z_2, \ldots, z_p)) = \exp(-1/\min(z_1, z_2, \ldots, z_p))$ and hence $\theta_p = V_Z(1, 1, \ldots, 1) = 1$. We see therefore that the value of θ_p between p and unity indicates the extend of extremal dependence.

Relating extremal coefficient and the χ statistic for asymptotic dependence

In the notation of Section 3.1, $\Pr[Z_l > z | Z_k > z] = \Pr[Z_l > z, Z_k > z]/\Pr[Z_k > z]$. But $\Pr[Z_l > z, Z_k > z] = 1 + \Pr[Z_l \le z, Z_k \le z] - \Pr[Z_k \le z] - \Pr[Z_l \le z]$ and $\Pr[Z_k > z] = 1 - \Pr[Z_k \le z]$. When z is large, $\Pr[Z_k \le z] = \exp(-1/z) \approx 1 - 1/z$ and $\Pr[Z_l \le z, Z_k \le z] = \exp(-\theta_{kl}/z) \approx 1 - \theta_{kl}/z$ so that

$$\Pr[Z_l > z | Z_k > z] \approx \frac{1 + (1 - \theta_{kl}/z) - (1 - 1/z) - (1 - 1/z)}{1 - (1 - 1/z)} = 2 - \theta_{kl}.$$

The constructive representation of MSPs

de Haan (1984) described MSPs using the so-called constructive representation, which provides a straightforward way to simulate from MSPs with arbitrary numbers of components and standard Fréchet margins. Following Wadsworth and Tawn (2012), an MSP is the maximum of multiple copies $\{W_i\}$ $(i \ge 1)$ of a random function W, each copy weighted using the value of a Poisson process $\{\rho_i\}$ $(i \ge 1)$. The MSP $Z(s)$ for s in spatial domain $\mathcal{S}$ is evaluated as

$$Z(s) = \mu^{-1} \max_i \{W_i^+(s)/\rho_i\}, \text{where } W_i^+ \text{is } \max\{W_i(s), 0\}.$$

The Poisson process ρ_i gives values on $(0, \infty)$. Without loss of generality we assume it has unit intensity, and can be constructed using standard exponential random variables (with distribution Exp(1)) as follows

$$\begin{aligned} \rho_i &= \varepsilon_1 \text{ where } \varepsilon_1 \sim Exp(1) \text{ for } i = 1, \\ &= \varepsilon_i + \rho_{i-1} \text{ where } \varepsilon_i \sim Exp(1) \text{ for } i > 1. \end{aligned}$$

The effect of the Poisson weighting is to make it increasingly unlikely that a value of $W_i(s)$ at large i will contribute to $Z(s)$. This means that we can safely terminate the construction simulation after a number of iterations. The random function $W(s)$ gives real values, and the expected value $E(W^+(s))$ of its positive part is μ, independent of location s. Once the function W is specified, μ can usually be evaluated in closed form, although we find it useful in general to use the empirical estimate $\hat{\mu}$ obtained directly from the simulation. In the current work, for all MSPs, $\mu = 1$ by construction. Different choices of $W(s)$ give different MSPs.

The Smith model: In one of the first models for spatial extremes, Smith (1990) proposed that $W_i(s)$ be a Gaussian density function centred at some s_i, with s_i sampled at random from a uniform distribution on $\mathcal{S}$. More generally we can sample s_i from any density f_S defined on $\mathcal{S}$, so that

$$W_i(s; s_i, \Sigma) = \varphi(s - s_i; \Sigma)/f_S(s_i)$$

where φ is the density of the standard Gaussian random variable. In oceanographic terms in two dimensions (with $\mathcal{S} = [s_{1\min}, s_{1\max}] \times [s_{2\min}, s_{2\max}]$), s_i could be the location of the centre of a storm, and f_S the density of rate of occurrence of storm events throughout $\mathcal{S}$. $W_i(s; s_i, \Sigma)$ would then characterise the influence of a storm centred at s_i on location s. If we assume s_i to be uniformly sampled on $\mathcal{S}$, $W_i(s; s_i, \Sigma)$ is simply

$$W_i(s; s_i, \Sigma) = \frac{1}{2\pi|\Sigma|^{1/2}} \frac{e^{-h'\Sigma^{-1}h/2}}{[s_{1max} - s_{1min}][s_{2max} - s_{2min}]}$$

where $h = s - s_i$ is the vector displacement of s from s_i, and Σ is a 2×2 covariance matrix. The elements of Σ define the "spatial shape of a storm event". The corresponding exponent measure V_{kl} between two locations s_k, s_l is given in the main text.

The Schlather model: The Schlather MSP makes use of Gaussian processes (Rasmussen and Williams, 2006); a Gaussian process is a collection of random variables, any finite number of which have a joint Gaussian distribution. Each $W_i(s)$ is now a random process rather than a deterministic function as in the Smith model. $\{W_i(s)\}$ are taken to be copies of a stationary standard Gaussian process $W(s)$ on $\mathcal{S}$, defined in terms of its correlation function $\tau(h) \in [0, 1]$ given by $\tau(h) = E[W(s + h)W(s)]$ for all $s, s + h \in \mathcal{S}$. $E[W(s)] = 0$ and $E[W^2(s)] = 1$ for the standard Gaussian process, and further $\tau(0) = 1$, and τ depends only on the vector displacement $h = s_l - s_k$ for two locations, rather than the absolute locations themselves. It is conventional to write

$$W(s) \sim \mathcal{GP}(0, \tau(h)).$$

One suitable functional form for $\tau(h)$ is $\exp(-h'\Sigma^{-1}h)$ for some covariance matrix Σ. For any pair of locations s_k, s_l the joint distribution of $W(s_k)$, $W(s_b)$ is then bivariate normal: $(W(s_a), W(s_b); h(\Sigma)) \sim N(0, \Omega(h))$, where $\Omega(h) = [1 \quad \tau(h); \tau(h) \quad 1]$. Moreover, the joint distribution of W on any finite set of locations is multivariate Gaussian with Ω defined analogously, providing a straightforward procedure to simulate copies $W_i(s)$, and hence to simulate the Schlather MSP.

The Brown-Resnick model: Simulation under the Brown-Resnick model is more complicated, and the literature generally focuses on approximate

Algorithm Simulating a realisation from a max-stable processes with unit Fréchet margins

Input: Upper bound $B > 0$ to terminate procedure. Function to sample from spatial process W. Finite set of locations $S \subseteq \mathcal{S}$ at which to simulate.

Output: One realisation $\{Z(s)\}$ of a max-stable process for $s \in S$.

for i=1,2,... **do**
  $\rho = \rho + E$, $E \sim \text{Exp}(1)$.
  $W_i(s) \sim W$ for all locations $s \in S$.
  $W_i^+(s) = \max(W_i(s), 0)$ for all s
  for $s \in S$ **do**
    $Z(s) = \max(Z(s), W_i(s)/\rho)$ for all s.
  end for
  if $B/\rho < \min(Z(s))$ **then**
    exit loop.
  end if
end for
$Z(s) = \mu^{-1} Z(s)$ for all s.
return $\{Z(s)\}$.

simulation techniques. Here, we choose to follow the approach of Dieker and Mikosch (2015) which provides exact simulations of Brown-Resnick random fields (developed from Brown and Resnick 1977) at a finite number of locations. Each $W_i(s)$ has the form

$$W_i(s_j) = \frac{\exp(\varepsilon_i(s_j) - \gamma(s_j - U_i))}{p^{-1}\sum_{k=1}^{p} \exp(\varepsilon_i(s_k) - \gamma(s_k - U_i))}$$

on a grid of locations $\{s_j\}_{j=1}^p \in \mathcal{S}$. $\{\varepsilon_i(s)\}$ are independent copies of a centred Gaussian process $\varepsilon(s)$ with stationary increments, with variance $\text{var}[\varepsilon(s)] = \sigma^2(s)$ and semi-variogram $\gamma(h) = (1/2)E[(\varepsilon(s+h) - \varepsilon(s))^2]$. $\{U_i\}$ are randomly chosen locations on $\mathcal{S}$. The assumption of stationary increments for $\varepsilon(s)$ implies that the statistical characteristics of $\varepsilon(s+h) - \varepsilon(s)$ do not depend on s; the statistical properties of the Gaussian process are thus uniquely defined by $\gamma(h)$ alone. Since we can assume $\varepsilon = 0$ at the origin of coordinates almost surely, by definition we have $\gamma(h) = E[(\varepsilon(h))^2]/2 = \sigma^2(h)/2$. We assume $\gamma(h) = (1/2)(h'\Sigma^{-1}h)^H$, for Hurst parameter $H \in (0, 1]$. When $H = 0.5$, $\varepsilon(s)$ is a Brownian motion (or Wiener process); when $H = 1$, the Brown-Resnick and Smith processes coincide. The corresponding covariance function is given by $\tau(s_k, s_l; \Sigma, H) = \frac{1}{2}\left((s_k^T\Sigma^{-1}s_k)^H + (s_l^T\Sigma^{-1}s_l)^H - ((s_l - s_k)^T\Sigma^{-1}(s_l - s_k))^H\right)$. An algorithm for simulation of one realisation from a Brown-Resnick process is provided below.

We note in passing that the geometric Gaussian process (Davison et al., 2012), a simplified form of the Brown-Resnick process using a stationary standard Gaussian process in place of the centred Gaussian process with stationary increments, provides much of the flexibility of the Brown-Resnick process without the computational concerns.

Bivariate densities for MSPs

The Smith and Brown-Resnick models: Padoan et al. (2010) derives the bivariate density to be

$$f_{kl}(z_k, z_l; h(\Sigma)) = \exp\left(-\frac{\Phi(w)}{z_k} - \frac{\Phi(v)}{z_l}\right)\left[\left(\frac{\Phi(w)}{z_k^2} + \frac{\varphi(w)}{az_k^2} - \frac{\varphi(v)}{az_i}z_l\right)\left(\frac{\Phi(v)}{z_l^2} + \frac{\varphi(v)}{az_l^2} - \frac{\varphi(v)}{az_i}z_l\right) + \left(\frac{v\varphi(w)}{a^2z_k^2z_l} + \frac{w\varphi(v)}{a^2z_iz_l^2}\right)\right]$$

Algorithm Exact method for simulation of realisation from Brown-Resnick random field.

Input: Fixed grid of locations $\{s_j\}$ on $\mathcal{S}$. Covariance function $\tau(s_k, s_l; \Sigma, H)$.

Output: Realisation $\{W_i(s_j)\}$ of Brown-Resnick process on grid with Fréchet margins.

Draw index i of shift location s_i at random from $1, 2, ..., p$.
Draw Gaussian realisation $\{z_j\} \sim \mathcal{GP}(0, \tau(s_k, s_l; \Sigma, H))$.
for j=1,2,...,p **do**
  $\gamma_j = (1/2)\left((s_j - s_i)'\Sigma^{-1}(s_j - s_i)\right)^H$.
  $Y_j = Z_j - \gamma_j$.
  $W(s_j) = \exp(Y_j)/(p^{-1}\sum_k \exp(Y_k))$.
end for
return $\{W_i(s_j)\}$.

where φ is the standard Gaussian density, $w = w(h) = m(h)/2 + \log(z_l/z_k)/m(h)$, and $v = v(h) = m(h) - w(h)$.

The Schlather model: The derivation of the Schlather derivative is more laborious. Eventually we obtain

$$f_{kl}(z_k, z_l; h(\Sigma)) = A\left[2 - W^{-1}(\tau(h)+1)\left(\frac{z_k - z_l}{z_k + z_l}\right)^2\right]$$

where $W = 1–2(\tau(h)+1)z_k z_l/(z_k + z_l)^2$ and $A = (1/2)W^{-\frac{1}{2}}(\tau(h)+1)/(z_k + z_l)^3$.

References

Brown, B.M., Resnick, S.I., 1977. Extreme values of independent stochastic processes. J. Appl. Probab. 14, 732–739.

Chandler, R.E., Bate, S., 2007. Inference for clustered data using the independence loglikelihood. Biometrika 94, 167–183.

Chavez-Demoulin, V., Davison, A., 2005. Generalized additive modelling of sample extremes. J. Roy. Stat. Soc. Ser. C. Appl. Stat. 54, 207–222.

Davison, A.C., Padoan, S.A., Ribatet, M., 2012. Statistical modelling of spatial extremes. Stat. Sci. 27, 161–186.

de Haan, L., 1984. A spectral representation for max–stable processes. Ann. Prob. 12, 1194–1204.

de Haan, L., Resnick, S.I., 1977. Limit theory for multivariate sample extremes. Z. Wahrscheinlichkeitstheorie verwandte Geb. 40, 317–337.

Dieker, A.B., Mikosch, T., 2015. Exact simulation of brown-resnick random fields at a finite number of locations. Extremes 18, 301–314.

Eastoe, E., Koukoulas, S., Jonathan, P., 2013. Statistical measures of extremal dependence illustrated using measured sea surface elevations from a neighbourhood of coastal locations. Ocean Eng. 62, 68–77.

Haario, H., Saksman, E., Tamminen, J., 2001. An adaptive metropolis algorithm. Bernoulli 7, 223–242.

Heffernan, J.E., Tawn, J.A., 2004. A conditional approach for multivariate extreme values. J. R. Stat. Soc. B 66, 497–546.

Heideman, J.C., Mitchell, D.A., 2009. Grid point pooling in extreme value analysis of hurricane hindcast data. J. Waterw. Port. Coast. Ocean Eng. 135, 31–38.

Huser, R., Davison, A.C., 2014. Space-time modelling of extreme events. J. Roy. Stat. Soc. B 76, 439–461.

Kereszturi, M., 2016. Assessing and Modelling Extremal Dependence in Spatial Extremes. PhD thesis. Lancaster University, U.K.

Kereszturi, M., Tawn, J., Jonathan, P., 2016. Assessing extremal dependence of north sea storm severity. Ocean Eng. 118, 242–259.

Mendez, F.J., Menendez, M., Luceno, A., Medina, R., Graham, N.E., 2008. Seasonality and duration in extreme value distributions of significant wave height. Ocean Eng. 35, 131–138.

Oceanweather, 2002. North European Storm Study User Group Extension and Reanalysis Archive. Oceanweather Inc.

Padoan, S.A., Ribatet, M., Sisson, S.A., 2010. Likelihood - based inference for max - stable processes. J. Am. Stat. Soc. 105, 263–277.

Rasmussen, C., Williams, C., 2006. Gaussian Processes for Machine Learning. MIT Press.

Ribatet, M., 2013. Spatial extremes: max-stable processes at work. J. de la Soc. Francaise de Statistique 154, 156–177.

Roberts, G.O., Rosenthal, J.S., 2009. Examples of adaptive mcmc. J. Comp. Graph. Stat. 18, 349–367.

Ross, E., Randell, D., Ewans, K., Feld, G., Jonathan, P., 2017. Efficient estimation of return value distributions from non-stationary marginal extreme value models using Bayesian inference. Ocean Eng. 142, 315–328.

Sartini, L., Cassola, F., Besio, G., 2015. Extreme waves seasonality analysis: an application in the Mediterranean Sea. J. Geophys. Res. Oceans 120, 6266–6288.

Schlather, M., 2002. Models for stationary max-stable random fields. Extremes 5, 33–44.

Smith, R. L., 1990. Max-stable processes and spatial extremes. Unpublished article, available electronically from www.stat.unc.edu/postscript/rs/spatex.pdf.

Smith, R.L., Tawn, J.A., Coles, S.G., 1997. Markov chain models for threshold exceedances. Biometrika 84, 249–268.

Sutcliffe, J.V., 1979. Obituary of Harold Edwin Hurst. Hydrol. Sci. Bull. 24, 539–541.

Varin, C., Reid, N., Firth, D., 2011. An overview of composite likelihood methods. Stat. Sin. 21, 5–42.

Wadsworth, J., Tawn, J., 2012. Dependence modelling for spatial extremes. Biometrika 99, 253–272.

Wadsworth, J.L., Tawn, J.A., Davison, A.C., Elton, D.M., 2017. Modelling across extremal dependence classes. J. Roy. Stat. Soc. C 79, 149–175.